

# Chemical composition of UV-bright star ZNG 4 in the globular cluster M13 <sup>★</sup>

S. Ambika<sup>1</sup>, M.Parthasarathy<sup>1</sup>, W.Aoki<sup>2</sup>, T.Fujii<sup>2,3</sup>, Y.Nakada<sup>4,5</sup>, Y.Ita<sup>4</sup>, and  
H.Izumiura<sup>6</sup>

<sup>1</sup> Indian Institute of Astrophysics, Koramangala, Bangalore - 560034, India

<sup>2</sup> National Astronomical Observatory, Mitaka, Tokyo 181-8588, Japan

<sup>3</sup> Faculty of Science, Kagoshima University, 1-21-35 Korimoto, Kagoshima, 890-0065,  
Japan

<sup>4</sup> Institute of Astronomy, The University of Tokyo, Mitaka, Tokyo, 181-0015, Japan

<sup>5</sup> Kiso Observatory, Institute of Astronomy, University of Tokyo, Mitake, Kiso, Nagano  
397-0101, Japan

<sup>6</sup> Okayama Astrophysical Observatory, National Astronomical Observatory, Kamogata,  
Okayama 719-0232, Japan

Received 20 May 2003 / Accepted 18 November 2003

**Abstract.** We present a detailed model-atmosphere analysis of ZNG 4, a UV-bright star in the globular cluster M13. From the analysis of a high resolution ( $R \approx 45,000$ ) spectrum of the object, we derive the atmospheric parameters to be  $T_{\text{eff}} = 8500 \pm 250$  K,  $\log g = 2.5 \pm 0.5$  and  $[\text{Fe}/\text{H}] = -1.5$ . Except for magnesium, chromium and strontium, all other even Z elements are enhanced with titanium and calcium being overabundant by a factor of 0.8 dex. Sodium is enhanced by a factor of 0.2 dex. The luminosity of ZNG 4 and its position in the color-magnitude diagram of the cluster indicate that it is a Supra Horizontal Branch (SHB) (post-HB) star. The underabundance of He and overabundances of Ca, Ti, Sc and Ba in the photosphere of ZNG 4 indicate that diffusion and radiative levitation of elements may be in operation in M 13 post-HB stars even at  $T_{\text{eff}}$  of 8500K. Detailed and more accurate abundance analysis of post-HB stars in several globular clusters is needed to further understand their abundance anomalies.

**Key words.** Stars: abundances – Stars: evolution – Stars: Population II – Stars: horizontal-branch – globular cluster : individual : M13 – Stars : individual : ZNG 4

---

<sup>★</sup> Based on observations obtained with the Subaru 8.2m Telescope, which is operated by the National Astronomical Observatory of Japan.

## 1. Introduction

The term "UV-bright stars" was introduced by Zinn et al.(1972) for stars in globular clusters that lie above the horizontal branch (HB) and are bluer than red giants. The name resulted from the fact that, in the U band, these stars were brighter than all other cluster stars. Further investigations showed that this group of stars consist of blue horizontal branch (BHB) stars, supra horizontal branch stars (SHB), post asymptotic giant branch stars (post-AGB), post-early AGB (P-EAGB) stars and AGB-manque stars. (de Boer 1985, 1987, Sweigart et al.1974, Brocato et al. 1990, Dorman et al. 1993 and Gonzalez & Wallerstein 1994)

To derive the chemical composition of UV-bright stars in globular clusters and to understand their evolutionary stages, we started a program to obtain high resolution spectra of these objects in selected globular clusters with the High Dispersion Spectrograph (HDS, Noguchi et al. 2002) of the 8.2m Subaru Telescope. We selected a few UV-bright stars in the globular cluster M13 from the papers of Zinn et al.(1972) and Harris et al.(1983) to derive their chemical composition. In this paper we report the analysis of a high resolution spectrum of the UV-bright star ZNG 4 (RA ( $16^h41^m37^s.528$ ) and DEC ( $+36^\circ30'43.86''$ ) (2000) ) (Zinn et al. 1972) in M13 as the first target of our program.

M13 (NGC 6205) is a nearby well-studied globular cluster with a distance modulus of  $(m - M)_0 = 14^m42$  and metallicity of  $[Fe/H] = -1.51$  (Kraft and Ivans 2003). The position of ZNG 4 in the color-magnitude diagram of M13 (Paltrinieri et al. 1998) is shown in Figure 1. Many of the globular clusters show a prominent gap in the blue tail of the HB, which is presumed to be due to differential mass loss on the Red Giant Branch (RGB). In M13 it is observed at  $T_{\text{eff}} = 10000\text{K}$  (Ferraro et al. 1997). High resolution spectroscopic studies of M13 BHB stars lying on either side of the gap were carried out by Peterson et al.(1983, 1995) and Behr et al.(1999, 2000a). They found anomalous photospheric abundances in BHB stars. These photospheric anomalies are most likely due to diffusion - the gravitational settling of helium and radiative levitation of the metal atoms in the stable atmosphere of hot stars. They found variations in the photospheric abundances and rotational velocities of BHB stars as a function of their effective temperatures.

## 2. Observations

We have obtained a high resolution ( $\frac{\lambda}{\Delta\lambda} \approx 45,000$ ) spectrum of ZNG 4 on 15th (UT:14h45m) April 2001 with the Subaru/HDS. The spectrum covering the wavelength range  $4142 \text{ \AA} - 6814 \text{ \AA}$  was obtained in an exposure time of 20 minutes. There was no moon light problem during the observations and the sky background in the data was close to zero. We neglected the sky background in our data reduction.

The data was bias-subtracted, trimmed, flat-fielded to remove pixel to pixel variations, converted to a one-dimensional spectrum, and normalized to the continuum using standard CCD

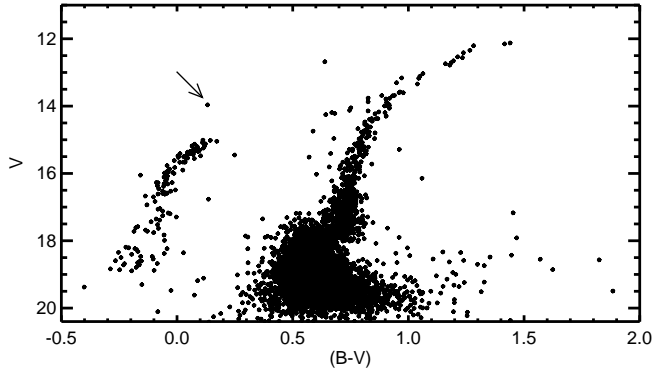


**Fig. 1.** Color magnitude diagram (CMD) of globular cluster M13 obtained by Paltrinieri et al.(1998). The arrow indicates the position of ZNG 4 in the CMD.

data reduction package (NOAO IRAF). The spectrum has an average signal to noise ratio of 35. The reference spectrum of thorium-argon was used for the wavelength calibration.

The various orders in our echelle spectrum of ZNG 4 have well defined continuum and the normalization of the continuum was carried out using the IRAF echelle spectra reduction programs. The continuum level in the adjacent echelle orders to those containing the Balmer lines was useful in defining the continuum in the Balmer line regions and the profiles were normalized with a polynomial fit.

### 3. Analysis

The spectral lines were identified using Moore's atomic multiplet table (1945). Equivalent widths of the absorption lines were measured using the routines available in the SPLOT package of IRAF. The equivalent widths were measured by Gaussian fitting to the observed profiles (and a multiple Gaussian fit to the blended lines such as the Mg II lines at 4481 Å) and are given in Table 1.

#### 3.1. Radial velocity

The radial velocity of ZNG 4 was derived from the wavelength shifts of many absorption lines. The average heliocentric velocity is found to be  $V_r = -257.56 \pm 1.08 \text{ km s}^{-1}$  which is in agreement with the value derived by Zinn (1974) ( $-253 \text{ km s}^{-1}$ ). It is also in agreement with the heliocentric velocities of M13 BHB stars derived by Behr et al. (1999) and Moehler et al. (2003).

#### 3.2. Atmospheric parameters

For the initial estimate of effective temperature, we looked for the published CCD photometry of the star. Recent CCD photometry of M13 was carried out by Rey et al. (2001). However the ZNG 4 area of the cluster was not included in their observations (Rey : private communication ). We used the published CCD photometry of ZNG 4 by Paltrinieri et al. (1998), who give,  $B=14.096$  and  $V=13.964$  .  $(B-V) = 0.132$  and  $E(B-V) = 0.02$  (Kraft and Ivans 2003) will yield

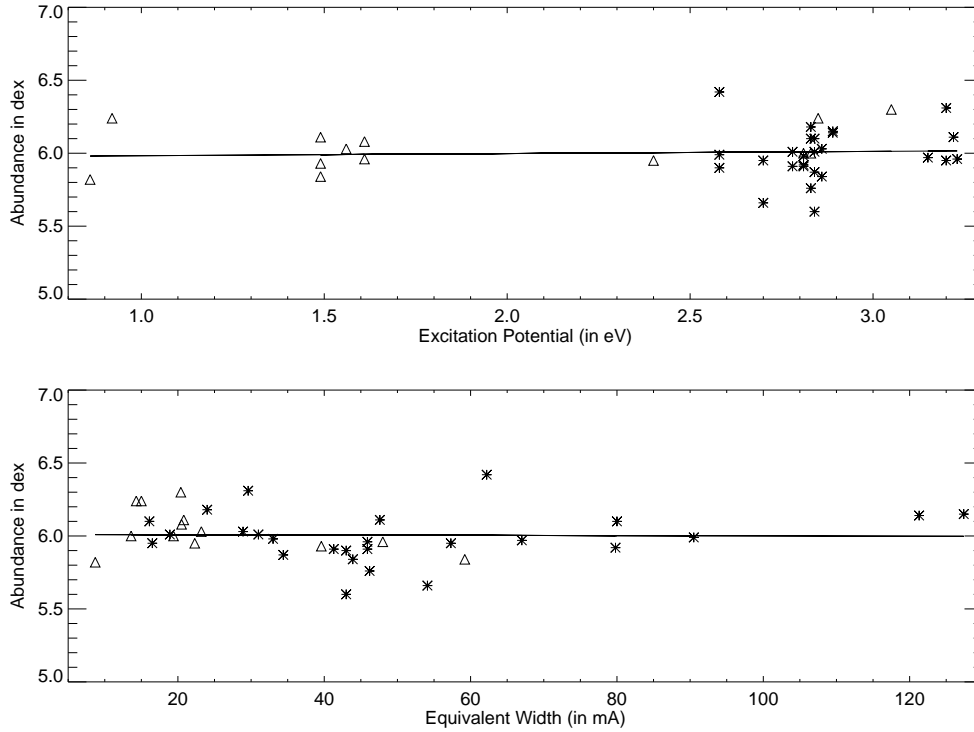


**Fig. 2.** Top figure is the plot of the abundances from Fe lines versus excitation potential of the lines. Figure at the bottom is the plot of the abundances from Fe lines versus their equivalent widths. Triangles represent the Fe I lines and stars denote the Fe II lines.

$(B - V)_0 = 0.112$  which corresponds to  $T_{\text{eff}} = 8373\text{K}$  (Flower 1996). However, the  $(B - V)_0$  and  $T_{\text{eff}}$  calibration given by Flower (1996) is for Population I stars.

For our analysis, excitation potential and oscillator strengths of the lines were taken from the Vienna Atomic Line Database ( <http://www.astro.univie.ac.at/~vald/> ). We employed the latest (2002) version of MOOG, an LTE stellar line analysis program (Snedden 1973) and Kurucz (1993) grid of ATLAS models. MOOG has been used successfully in the analysis of the spectra of warmer stars with  $T_{\text{eff}} = 7900\text{K}$  (Preston and Sneden 2000).

We have also analyzed the spectra using the Kurucz WIDTH program (Kurucz CDROM 13, 1993) for verification. We used the line list obtained using version 43 of the Synspec code of Hubeny and Lanz which is distributed as part of their TLUSTY model atmosphere program. ( <http://tlusty.gsfc.nasa.gov/Synspec43/synspec-line.html> ) and also the information from the Kurucz linelist ( <http://kurucz.harvard.edu/linelists.html> ).

The value of effective temperature was obtained by the method of excitation balance, forcing the slope of abundances from Fe I lines versus excitation potential to be zero. The surface gravity was then set by ionization- equilibrium, forcing abundances obtained from neutral (Fe I) and ionized (Fe II) species to be equal. The microturbulent velocity was estimated by demanding that there should be no dependence of the Fe I abundance upon equivalent widths of Fe I lines.

The plots of the abundances versus excitation potentials and abundances versus equivalent widths in the case of Fe I and Fe II lines are shown in Figure 2. Such plots were made by

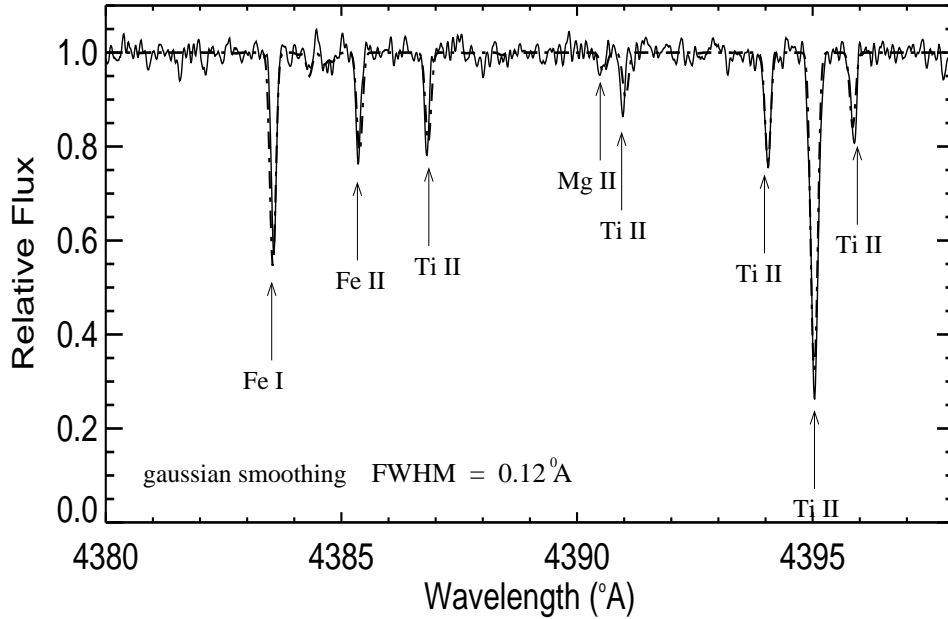


**Fig. 3.** Synthetic spectrum calculated with the atmospheric parameters ( $T_{\text{eff}} = 8500$  K,  $\log g = 2.5$ ,  $V_t = 2.5$  km s $^{-1}$ ) and abundances (Tables 1 and 2) is overplotted on the observed spectrum in the 4380 Å - 4400 Å region.

varying the  $T_{\text{eff}}$ ,  $\log g$  and  $V_t$  in steps of 250 K, 0.5 and 0.5 km s $^{-1}$  respectively to estimate the uncertainties in these parameters.

From our analysis, we find that  $T_{\text{eff}} = 8500$ K,  $\log g = 2.5$  and  $V_t = 2.5$ km s $^{-1}$  fit the data best (Figure 2). From the abovementioned method of analysis we find the uncertainties in  $T_{\text{eff}}$  to be 250 K,  $\log g = 0.5$  dex and  $V_t = 0.5$  km s $^{-1}$ . Uncertainties in derived abundances as a result of errors in the determination of the parameters and errors in the measurements of equivalent widths are found to be of the order of 0.2 dex.

Using the derived atmospheric parameters and abundances, a synthetic spectrum was generated and plotted over the observed spectrum for verification. The observed and synthetic spectra were found to match well with the above mentioned atmospheric parameters and the final abundances are given in Tables 1 and 2. A region of the observed and synthetic spectrum is shown in Figure 3. The abundances derived using MOOG (Tables 1 and 2) are in good agreement with the abundances derived using the WIDTH (Table 2).

### 3.3. Balmer Lines

We tried to estimate the  $T_{\text{eff}}$  and  $\log g$  from the analysis of Balmer lines in the spectrum of ZNG4 using the Kurucz spectral atlas for Balmer lines (Kurucz CDROM 13, 1993).

We could not get a satisfactory fit between the observed and theoretical Balmer line profiles with the atmospheric parameters  $T_{\text{eff}} = 8500$  K,  $\log g = 2.5$ ,  $V_t = 2.5$  km s $^{-1}$  and  $[\text{Fe}/\text{H}] = -1.5$

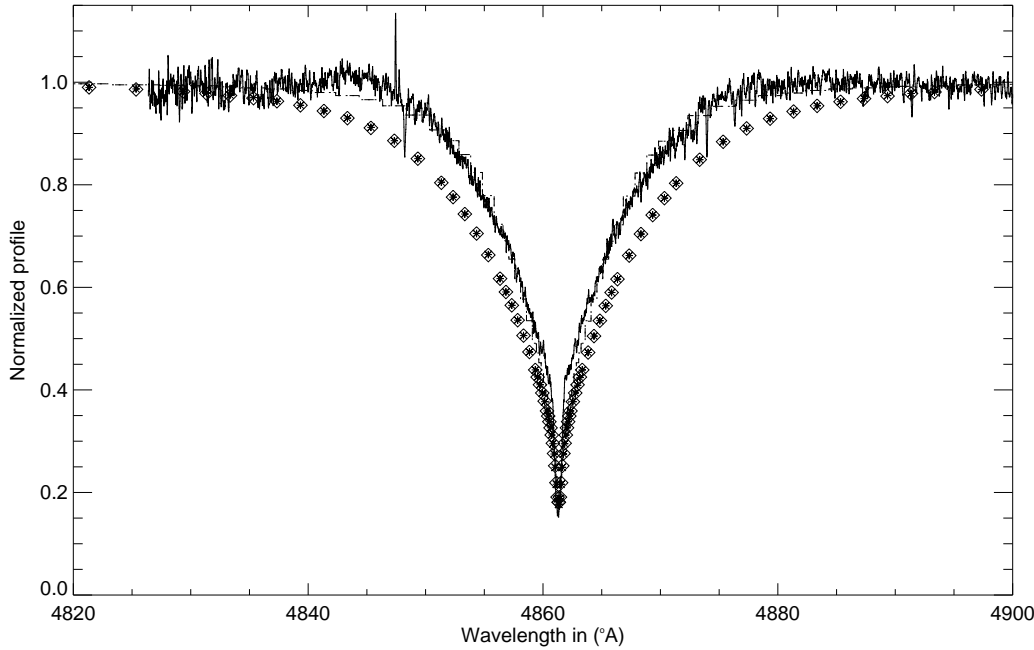


**Fig. 4.** Observed  $H_{\beta}$  profile compared with theoretical  $H_{\beta}$  profiles for 2 different model atmospheric parameters. Dots and dashes represent the model with  $T_{\text{eff}} = 8750$  K,  $\log g = 2.0$ ,  $[M/H] = -1.5$  and  $V_t = 2.0$  km  $s^{-1}$  which fit the profile best. Open diamonds and asterisks represent the model  $T_{\text{eff}} = 8500$  K,  $\log g = 2.5$ ,  $[M/H] = -1.5$  and  $V_t = 2.5$  km  $s^{-1}$ , which does not fit the observed profile. No noticeable differences were observed in the theoretical  $H_{\beta}$  profiles by considering ANOVER models for the same atmospheric parameters and are shown by dashes for the first set of parameters and asterisk in the case of second set of parameters.

. We also tried models that take into account the alpha element enhancements and no convective overshooting (ANOVER models: [HTTP://KURUCZ.harvard.edu/grids/gridm15ANOVER/bm15ak2nover.dat](http://kurucz.harvard.edu/grids/gridm15ANOVER/bm15ak2nover.dat)). However, the profiles were found to be similar (Figure 4). The best fit to  $H_{\beta}$  profile was obtained with the parameters  $T_{\text{eff}} = 8750$  K,  $\log g = 2.0$ ,  $V_t = 2.0$  km  $s^{-1}$  and  $[Fe/H] = -1.5$  (Figure 4). However, the excitation balance and ionization equilibrium for Mg and Fe lines could not be achieved with the above parameters (see the last column in Table 2) and the abundances of Mg I, Mg II and Fe I, Fe II were found to differ significantly (Table 2). Therefore, we chose the model atmosphere determined from the analysis of metal lines (ie  $T_{\text{eff}} = 8500$  K,  $\log g = 2.5$ ,  $V_t = 2.5$  km  $s^{-1}$  and  $[Fe/H] = -1.5$ ) to represent the atmosphere of the star.

The problem of fitting Balmer line profiles of HB stars has been mentioned by Grundahl et al. (1999) (and references therein). For stars being more luminous than HB stars, mass loss and/or extended atmosphere may influence the Balmer line profiles (Vink & Cassisi, 2002).

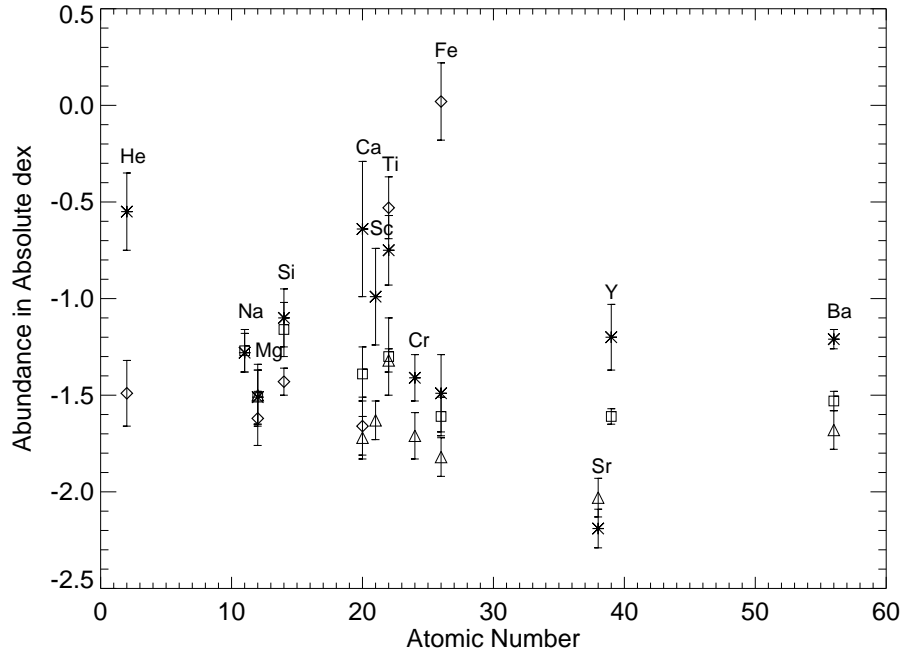


**Fig. 5.** The abundances of different elements in ZNG 4 (represented by asterisk) compared with M13/ J11 ( BHB star; triangles), M13/WF4-3485 (hot BHB star; diamonds) and that of M13/ L262 (RGB star; squares) with their error bars (Table 3). In the cases where only upper limit of the abundances are given (3rd and 4th column of Table 3), those elements are not shown in the above figure. Average abundances of Y and Ba in M13 RGB stars are from Armosky et al. (1994).

#### 4. Results

The mean abundances of ZNG 4 relative to the Sun (Anders and Grevesse 1989) are given in Table 2, together with the number of lines used in the analysis and the standard deviation of abundances estimated from individual species.

Analysis of Mg lines gives  $[Mg/H] = -1.5$  which is the same as the M13 cluster metallicity. (The equivalent widths of the Mg II lines at 4481 Å (Table 1) were obtained by a multiple gaussian fit to the lines in the observed spectrum). Silicon is overabundant compared to iron ( $[Si/Fe] = +0.4$ ). Calcium and titanium are found to be overabundant ( $[Ca/Fe] = +0.8$  and  $[Ti/Fe] = +0.75$ ). There is a 0.5 dex difference in the abundances derived from the Ca I lines at 4226.73 Å and 4454.78 Å (Table 1). However, the abundance of Ca derived from the Ca II line at 5019.97 Å is in agreement with that derived from the Ca I 4454.78 Å line. The reason for the deviation in the abundance derived from the Ca I 4226.73 Å line is not clear. It may be due to the relatively low signal to noise ratio of the data around this wavelength range. There seems to be no interstellar contribution to the Ca II line. Since the star has a radial velocity of  $-257 \text{ km s}^{-1}$ , the stellar lines are well separated from the lines of interstellar origin. The abundance of Cr and Fe ( $[Fe/H] = -1.48$  and  $[Cr/Fe] = +0.09$ ) are found to be close to the metallicity of the cluster. On the other hand, Sc is found to be overabundant ( $[Sc/Fe] = 0.51$ ). Na lines show an

overabundance of 0.2 dex. We have detected one line of Sr II, two lines of Y II and two lines of Ba II. Sr seems to be underabundant ( $[\text{Sr}/\text{Fe}] = -0.70$ ), while Y and Ba are overabundant ( $[\text{Y}/\text{Fe}] = +0.29$  and  $[\text{Ba}/\text{Fe}] = +0.28$ ).

We have detected the He I line at  $4471.47 \text{ \AA}$ , which yields an abundance of  $\log \epsilon(\text{He}) = 10.44$  which implies an underabundance of 0.55 dex compared to the solar value. This is in agreement with the underabundance of He found in hot BHB stars (Moehler, 1999, Moehler et al. 2003).

We have not detected C, N and O lines in our spectrum of ZNG 4. Assuming an equivalent width of  $5 \text{ m\AA}$  as the detectable limit in our spectrum of ZNG 4, we find the upper limit of  $[\text{C}/\text{Fe}]$  to be  $+0.32$  dex (based on the C I  $5052.17 \text{ \AA}$  line), that of  $[\text{N}/\text{Fe}]$  to be  $+1.15$  dex (based on the N I  $4214.80 \text{ \AA}$  line) and that of  $[\text{O}/\text{Fe}]$  to be  $+0.01$  dex (based on the O I  $6156.78 \text{ \AA}$  line). Globular cluster stars show anticorrelation of sodium and oxygen abundances (Kraft et al. 1997). In ZNG 4 we find enhancement of sodium, therefore we expect an underabundance of oxygen. Also star to star abundance variations in the light elements C, N, O, Na, Mg and Al occur among the bright giants of a number of globular clusters (Ivans et al. 1999). The absence of C, N and O lines in our spectrum of ZNG 4 may be due to the underabundance of these elements. A much higher resolution and high signal to noise ratio spectrum of ZNG 4 may reveal the lines of C, N and O lines if present.

## 5. Discussion and Conclusions

The chemical composition of ZNG 4 shows significant deviations in element abundances from the expected metallicity of M13. Ti, Ca, Sc and Ba are found to be relatively overabundant (Figure 5) compared to RGB stars and cool BHB stars of M13, whereas the abundances of Mg, Cr and Fe are in agreement with the cluster metallicity.

From a study of 22 M13 G-K giants, Kraft et al. (1993, 1997) found the abundances of Fe, Sc, V and Ni to be  $[\text{Fe}/\text{H}] = -1.49$ ,  $[\text{Sc}/\text{Fe}] = -0.10$ ,  $[\text{V}/\text{Fe}] = 0.00$  and  $[\text{Ni}/\text{Fe}] = -0.04$ . They found Ca and Ti to be mildly overabundant ( $[\text{Ca}/\text{Fe}] = +0.24$  and  $[\text{Ti}/\text{Fe}] = +0.29$ ). Si was overabundant by  $+0.34$  dex. Study of M13 giants by Armosky et al. (1994) yields the average abundance of Fe, Y and Ba :  $[\text{Fe}/\text{H}] = -1.49$ ,  $[\text{Y}/\text{Fe}] = -0.12$  and  $[\text{Ba}/\text{Fe}] = -0.04$ , whereas in ZNG 4 we find significant overabundance of Ca, Sc, Ti, Y and Ba compared to that found in M13 giants. Also, overabundance of Na [ $+0.2$  dex] and absence of O lines support the anticorrelation of Na and O abundances found in M13 giants (Kraft et al. 1997).

Behr et al. (1999) have studied the BHB stars in M13 on either side of the HB gap. They find the photospheric compositions and stellar rotation rates to vary strongly as a function of  $T_{\text{eff}}$  of the stars. Among the cooler stars in their sample, at  $T_{\text{eff}}$  of  $8500\text{K}$ , the metal abundances are in rough agreement with the canonical cluster metallicity and the hotter stars with  $T_{\text{eff}}$  greater than  $10000\text{K}$  show a deficiency of He and enhancement of Fe, Ti, Cr by a factor of 300. However, Mg remains at the canonical cluster metallicity. In ZNG 4 also, Mg abundance is in agreement with the M13 metallicity. Abundances similar to that found in BHB stars of M13 were also found in



BHB stars of M15 (Behr et al. 2000b) and BHB stars of NGC 6752 (Glaspy et al. 1989, Moehler et al. 1999). The abundance anomalies in these BHB stars are most likely due to diffusion - the gravitational settling of helium (Greestein et al. 1967) and radiative levitation of metal atoms (Michaud et al. 1983). Rotational velocities ( $v \sin i$ ) appear to have a bimodal distribution in cooler BHB stars, whereas the hotter BHB stars with  $T_{\text{eff}}$  greater than 10000K are found to be slow rotators.

However, the abundances and rotational velocity of ZNG 4 are contrary to what is expected for stars on the red side of the HB gap at 11,000 K. It is a slow rotator ( $v \sin i = 7 \text{ km sec}^{-1}$ ). It shows underabundance of He and overabundances of Ti, Ca, Sc and Ba. In Table 3 and Figure 5, we have compared the abundances of ZNG 4 with the abundances of M13 BHB stars of  $T_{\text{eff}}$  7681 K (J 11) and  $T_{\text{eff}}$  12,750 K (WF4-3485) (Behr, 2000c) and with the abundances of the RGB star L262 (Cavallo and Nagar, 2000). In Table 3, the last column shows the mean RGB abundances in M13, where elements from Na to Fe are taken from Kraft et al. (1997) and Y and Ba abundances are from Armosky et al. (1994). It is evident from the abundances listed in Table 3 and from Figure 5 that ZNG 4 shows overabundance of metals compared to that of a M13 RGB star and also when compared to that of a M13 BHB star of similar temperature. These results indicate that in ZNG4, diffusion and radiative levitation of elements may be in operation. Slowly rotating HB stars are also seen on the cooler side of HB gap, but abundance anomalies start from 11,000 K (Moehler et al. 1999, Behr et al. 2000b). This implies that ZNG 4 may have the properties of the stars on the blue side of the HB gap although it has  $T_{\text{eff}}$  of 8500 K. In this regard, more accurate determination of abundances of these elements in ZNG 4 and similar stars in M13 is needed to confirm our results and conclusions.

This may be explained in two ways. One is that, for some stars in M13, the onset of diffusion seems to start at lower  $T_{\text{eff}}$  ( $\approx 8500 \text{ K}$ ). The other argument would be that the star has evolved from the blue side of the HB gap and is moving towards the red with higher luminosity as indicated by the post-HB evolutionary tracks of Gingold (1976) and Dorman et al. (1993).

The BHB stars hotter than 11500K typically show strong photospheric helium depletions due to gravitational settling (Moehler et al. 2000 & 2003). The calculations of Michaud et al. (1983) indicate that helium depletion should be accompanied by photospheric enhancement of metals, since the same stable atmosphere that permits gravitational settling also permits the levitation of elements with large radiative cross sections. The depletion of helium and overabundance of some of the metals in the photosphere of ZNG 4 is in qualitative agreement with the calculations of Michaud et al. (1983).

Recently, Turcotte et al. (1998) and Richer et al. (2000) made diffusion simulations to explain the abundance patterns of chemically peculiar A and F stars. Their predicted abundance patterns are qualitatively similar to that found in ZNG 4. However, none of the recent diffusion studies treated the cases of BHB stars and post-HB stars. This phenomenon may be related to the disappearance of surface convection and hence to the formation of a stable stellar atmospheres. HB stars and post-HB stars cooler than  $T_{\text{eff}} = 6300\text{K}$  have deep convective envelopes (Sweigart

2002). Hotter than this temperature the envelope convection breaks into distinct shells associated with the ionization of H and He. Note that the surface convection disappears at 11000K (Sweigart 2002) and BHB stars hotter than this show moderate to severe abundance anomalies.

ZNG 4 has a V magnitude of 13.964 (Paltrinieri et al. 1998). Considering the distance modulus of M13 to be 14.42 and  $E(B - V)$  towards M13 to be 0.02 (Kraft and Ivans 2003), we estimated the absolute magnitude ( $M_v$ ) of the star to be  $-0.522$ . For stars with  $T_{\text{eff}}$  around 8500 K, the bolometric correction (BC) is negligible (Flower 1996). Considering  $BC = 0$ , we get the bolometric magnitude ( $M_{\text{bol}}$ ) to be  $-0.522$ , which corresponds to a luminosity of  $127 L_{\odot}$  [ $\log \frac{L}{L_{\odot}} = 2.18$ ]. Using the equation connecting the mass, effective temperature and bolometric magnitude, we find the surface gravity,  $\log g = 2.6$  (assuming the mass of ZNG 4 to be  $0.5 M_{\odot}$ ), which agrees well with the value estimated from the analysis of the spectrum of ZNG 4.

The post-AGB star Barnard 29 [ $\log \frac{L}{L_{\odot}} = 3.3$ ] which is a member of M13 is more luminous than ZNG 4. The abundance pattern of ZNG 4 is very different from that of the post-AGB star Barnard 29 (Conlon et al. 1994, Moehler et al. 1998). The M13 BHB stars with  $T_{\text{eff}}$  around 8500 K have a luminosity of about  $40 L_{\odot}$ , whereas ZNG 4 is more luminous by about a factor of 3, which indicates that ZNG 4 can be classified as a supra horizontal branch star (post-HB). Stars that lie 1.5 magnitude above the HB stars are classified as supra horizontal branch (SHB) stars in the photometric studies of M13 (Zinn 1974) and NGC 6522 (Shara et al. 1998). No detailed abundance analysis of SHB stars in globular clusters is available to compare with the abundances of ZNG 4.

Since ZNG 4 is a post-HB star and it has evolved from a hot BHB star stage and may have had severe abundance anomalies similar to those found in the hot BHB stars of M13 (Table 3). The present  $T_{\text{eff}} = 8500\text{K}$  of ZNG 4 indicates that thin layers of subsurface convection if present may have diluted the severe abundance anomalies due to diffusion and radiative levitation that took place during its hot BHB stage of evolution. It is important to derive the chemical composition of a significant sample of post-HB stars hotter than 11000K and much cooler than 11000K to further understand the role of diffusion, radiative levitation, rotation and convection during the post-HB stage of evolution.

*Acknowledgements.* We would like to thank Dr. B.Dorman and Dr.B.Behr for helpful information on M13 BHB stars, Dr. F.R.Ferraro for kindly providing the table of B and V magnitudes of M13 cluster stars and the referee Dr.S.Moehler for helpful comments.

## References

- Anders, E., Grevesse, N., 1989, *Geochim. Cosmochim. Acta*, 53, 197  
 Armosky, B. J., Sneden, C., Langer, G. E., Kraft, R. P., 1994, *AJ*, 108, 1364  
 Behr, B. B., Cohen, J. G., McCarthy, J. K., Djorgovski, S. G., 1999, *ApJ*, 517L, 135  
 Behr, B. B., Djorgovski, S. G., Cohen, J. G., McCarthy, J. K., Cote, P., Piotto, G., Zoccali, M., 2000a, *ApJ*, 528, 849  
 Behr, B.B, Cohen, J., G., McCarthy, J.K., 2000b, *ApJ*, 531, L37

- Behr, B.B., 2000c, PhD, Thesis, California Institute of Technology.
- Brocato, E., Matteucci, F., Mazzitelli, I., Tornambe, A., 1990, *ApJ*, 349, 458
- Cavallo, R. M., Nagar, N. M., 2000, *AJ*, 120, 1364
- Conlon, E.S., Dufton, P. L., Keenan, F. P., 1994, *A&A*, 290, 897
- Cudworth, K. M., Monet, D. G., 1979, *AJ*, 84, 774
- de Boer, K.S., 1985A & A, 142, 321
- de Boer, K. S., 1987, The second conference on faint blue stars, IAU colloquium, No.95, p95, L.Davis Press
- Dorman, B., Rood, R. T., O'Connell, R. W., 1993, *ApJ*, 419, 596
- Flower, P. J., 1996, *ApJ*, 469, 355
- Ferraro, F. R., Paltrinieri, B., Fuci Pecci, F., Dorman, B., Rood, R.T., 1997, *ApJ*, 500, 311
- Gingold, R. A., 1976, *ApJ*, 204, 116
- Glaspay, J.W., Michaud G., Moffat A.F.J., Demers S., 1989, *ApJ*, 339, 926
- Greenstein, G. S., Truran, J. W., Cameron, A. G. W., 1967, *Nature*, 213, 871
- Grundahl, F., Catelan, M., Landsman, W. B., et al., 1999, *ApJ*, 524, 242
- Gonzalez, G., Wallerstein, G., 1994, *AJ*, 108, 1325
- Harris, H. C., Nemec, J. M., Hesser, J. E., 1983, *PASP*, 95, 256
- Ivans, I. I., Sneden, C., Kraft, R. P., et al., 1999, *ApJ*, 118, 1273
- Kraft, R. P., Sneden, C., Langer, G.E., Shetrone, M. D., 1993, *AJ*, 106, 1490
- Kraft, R. P., Sneden, C., Smith, G. H., Shetrone, M. D., Langer, G. E., Pilachowski, C. A., 1997, *AJ*, 113, 279
- Kraft, R. P., Ivans, I. I., 2003, *PASP*, 115, 143
- Kurucz, R. L., 1993, (Kurucz CD-ROMS, Cambridge: Smithsonian Astrophys. Obs.)
- Michaud, G., Vauclair, G., Vauclair, S., 1983, *ApJ*, 267, 256
- Moehler, S., Heber, M., Lemke, M., Napiwotzki, R., 1998, *A&A*, 339, 537
- Moehler, S., 1999, *Reviews in Modern Astronomy*, 12, p281
- Moehler, S., Sweigart, A.V., Landsman, W.B., Heber, U., Catelan, M., 1999, *A & A*, 346, L1
- Moehler, S., Sweigart, A.V., Landsman, W.B., Heber, U., 2000 *A & A*, 360, 120
- Moehler, S., Landsman, W. B., Sweigart, A. V., Grundahl, F., 2003, *A & A*, 405, 135
- Moore, C. E. 1945, *A Multiplet Table of Astrophysical Interest, Part I, Table of Multiplets*, revised ed. (Princeton: Princeton Univ. Obs.)
- Noguchi, K., Aoki, W., Kawanomoto, S., et al., 2002, *PASJ*, 54, 855
- Paltrinieri, B., Ferraro, F. R., Carretta, E., Fusi Pecci, F., 1998, *MNRAS*, 293, 434
- Peterson, R. C., 1983, *ApJ*, 275, 737
- Peterson, R. C., Rood, R.T., & Crocker, D.A, 1995, *ApJ*, 453, 21
- Preston, G. W., Sneden, C., 2000, *AJ*, 120, 1014
- Rey, S-C., Yoon, S-J., Lee, Y-W., Chaboyer, B., Sarajedini, A., 2001, *AJ*, 122, 3219
- Richer J., Michaud G., Turcotte S., 2000, *ApJ* 529, 338
- Shara, M. M., Drissen, L., Rich, R. M., Paresce, F., King, I. R., Meylan, G., 1998, *ApJ*, 495, 796
- Sneden, C., 1973, *ApJ*, 184, 839
- Sweigart, A. V., Mengel, J. G., Demarque, P., 1974, *A & A*, 30, 13
- Sweigart A.V., 2002, *IAU Highlights of Astronomy* 12, 293
- Turcotte S., Richer J., Michaud G., 1998, *ApJ* 504, 559
- Vink, J. S., Cassisi, S., 2002, *A&A*, 392, 553

Zinn, R. J., Newell, E. B., Gibson, J. B., 1972, A & A, 18, 390

Zinn, R. J., 1974, ApJ, 193, 593

**Table 1.** Data for spectral lines measured in the spectrum of ZNG 4 in M13

$\lambda_{lab}$ (in Å)	LEP (eV)	log gf	EW ( $m\text{Å}$ )	log $\epsilon$
He I				
4471.47	20.96	-0.278	11.3	10.44
Na I				
5889.95	0.00	0.117	63.9	5.05
5895.92	0.00	-0.184	40.6	5.04
Mg I				
5167.32	2.71	-1.030	31.9	6.19
5172.68	2.71	-0.402	70.2	6.09
5183.60	2.72	-0.180	85.8	6.07
Mg II				
4481.13	8.86	0.740	104.1	6.12
4481.32	8.86	0.590	80.0	5.92
Si II				
5041.02	10.07	0.291	27.5	6.59
5055.98	10.07	0.593	25.5	6.24
6347.11	8.12	0.297	84.2	6.49
6371.37	8.12	-0.003	64.1	6.48
Ca I				
4226.73	0.00	0.265	76.7	5.21
4454.78	1.90	0.335	27.7	5.71
Ca II				
5019.97	7.51	-0.501	18.6	5.77
Sc II				
4246.82	0.32	0.242	54.5	1.58
4314.08	0.62	-0.096	47.8	2.03
4320.73	0.60	-0.252	49.7	2.21
4325.00	0.59	-0.442	35.9	2.18
4374.46	0.62	-0.418	39.8	2.23
4400.39	0.60	-0.536	32.3	2.21
4415.56	0.59	-0.668	31.5	2.32
Ti II				
4161.53	1.08	-2.160	20.8	4.27
4163.65	2.59	-0.210	76.3	4.22
4171.91	2.60	-0.270	75.0	4.27
4287.87	1.08	-1.820	38.8	4.26
4290.22	1.17	-0.930	91.1	4.16
4294.10	1.08	-0.880	95.2	4.12
4300.05	1.18	-0.490	129.9	4.43
4301.91	1.16	-1.200	78.7	4.25
4307.86	1.17	-1.100	62.6	3.93

**Table 1.** continued

$\lambda_{lab}$ (in Å)	LEP (eV)	log gf	EW ( $m\text{Å}$ )	log $\epsilon$
Ti II				
4312.86	1.18	-1.090	77.5	4.13
4314.98	1.16	-1.120	69.8	4.04
4320.96	1.17	-1.900	43.4	4.47
4330.24	2.05	-1.800	21.6	4.57
4330.69	1.18	-2.060	24.3	4.30
4344.29	1.08	-1.930	19.8	3.99
4350.83	2.06	-1.810	12.6	4.32
4367.66	2.59	-0.870	34.9	4.28
4386.84	2.60	-0.940	27.2	4.21
4391.03	1.23	-2.240	19.2	4.38
4394.05	1.22	-1.770	37.7	4.28
4395.03	1.08	-0.510	142.4	4.62
4395.85	1.24	-1.970	31.7	4.39
4399.77	1.24	-1.220	78.3	4.31
4407.68	1.22	-2.430	10.4	4.27
4411.07	3.10	-0.670	23.0	4.18
4417.72	1.17	-1.230	76.0	4.23
4418.33	1.24	-1.990	25.0	4.27
4421.94	2.06	-1.580	14.6	4.16
4443.79	1.08	-0.700	118.3	4.33
4450.48	1.08	-1.510	56.7	4.20
4464.45	1.16	-1.810	39.8	4.31
4488.33	3.12	-0.510	40.0	4.36
4529.47	1.57	-1.650	27.1	4.21
4533.97	1.24	-0.540	126.3	4.42
4549.62	1.58	-0.220	102.1	3.89
4563.76	1.22	-0.790	108.1	4.32
4571.97	1.57	-0.230	69.9	3.42
4589.96	1.24	-1.620	38.7	4.14
4763.88	1.22	-2.360	18.9	4.47
4779.98	2.05	-1.260	32.9	4.24
4798.52	1.08	-2.670	12.9	4.49
4805.09	2.06	-0.960	52.1	4.24
4874.01	3.10	-0.900	18.0	4.27
4911.19	3.12	-0.650	28.4	4.28
5129.15	1.89	-1.300	33.4	4.17
5154.07	1.57	-1.780	26.9	4.29
5185.91	1.89	-1.370	26.2	4.10
5188.68	1.58	-1.050	68.5	4.20

**Table 1.** continued

$\lambda_{lab}$ (in Å)	LEP (eV)	log gf	EW ( $m\text{Å}$ )	log $\epsilon$
Ti II				
5226.54	1.57	-1.230	52.1	4.16
5336.77	1.58	-1.630	31.9	4.25
5381.02	1.57	-1.970	21.9	4.38
Cr II				
4554.99	4.07	-1.282	14.8	4.40
4558.65	4.07	-0.449	44.5	4.18
4588.20	4.07	-0.627	34.6	4.20
4616.63	4.07	-1.361	15.0	4.48
4618.80	4.07	-0.840	26.1	4.25
4634.07	4.07	-0.990	19.1	4.23
4824.13	3.87	-0.970	20.6	4.11
5237.33	4.07	-1.160	13.0	4.21
Fe I				
4143.87	1.56	-0.511	23.2	6.03
4199.10	3.05	0.155	20.4	6.30
4202.03	1.49	-0.708	20.8	6.11
4260.47	2.40	0.109	22.3	5.95
4271.76	1.49	-0.164	39.6	5.93
4325.76	1.61	0.006	48.0	5.96
4383.55	1.49	0.200	59.2	5.84
4415.12	1.61	-0.615	20.5	6.08
4891.49	2.85	-0.112	15.0	6.24
4920.50	2.83	0.068	13.6	6.00
4957.60	2.81	0.233	19.4	6.00
5269.54	0.86	-1.321	8.7	5.82
5328.04	0.92	-1.466	14.3	6.24
Fe II				
4173.46	2.58	-2.740	62.2	6.42
4178.86	2.58	-2.500	43.0	5.90
4233.17	2.58	-1.900	90.5	5.99
4296.57	2.70	-3.010	16.5	5.95
4351.77	2.70	-2.020	54.1	5.66
4385.39	2.78	-2.680	31.0	6.01
4416.83	2.78	-2.410	41.3	5.91
4489.18	2.83	-2.970	24.0	6.18
4491.40	2.86	-2.700	28.9	6.03
4508.29	2.86	-2.250	43.9	5.84
4515.34	2.84	-2.450	34.4	5.87
4520.22	2.81	-2.600	33.0	5.98

**Table 1.** Continued

$\lambda_{lab}$ (in Å)	LEP (eV)	log gf	EW ( $m\text{Å}$ )	log $\epsilon$
Fe II				
4522.63	2.84	-2.030	43.0	5.60
4549.47	2.83	-2.020	80.0	6.10
4555.89	2.83	-2.160	46.2	5.76
4576.34	2.84	-2.920	18.9	6.01
4582.84	2.84	-3.090	16.1	6.10
4583.84	2.81	-1.860	79.8	5.92
4629.34	2.81	-2.330	45.9	5.91
4923.93	2.89	-1.320	121.3	6.14
5018.44	2.89	-1.220	127.4	6.15
5169.03	2.89	-1.303	134.4	6.37
5197.58	3.23	-2.100	45.9	5.96
5234.62	3.22	-2.230	47.6	6.11
5276.00	3.20	-1.940	57.3	5.95
5316.61	3.15	-1.850	67.0	5.97
5362.87	3.20	-2.739	29.6	6.31
6456.38	3.90	-2.100	45.8	6.46
Sr II				
4215.52	0.00	-0.145	19.8	0.71
Y II				
4177.53	0.41	-0.160	8.98	1.09
4374.94	0.41	0.160	11.10	0.86
Ba II				
4554.03	0.00	0.170	17.03	0.95
4934.08	0.00	-0.150	8.042	0.88



**Table 2.** Chemical composition of ZNG 4 in M13

Element	no of lines	$T_{\text{eff}} = 8500 \text{ K}, \log g = 2.5$ $V_t = 2 \text{ km s}^{-1}$ and $[\text{Fe}/\text{H}] = -1.5$ MOOG		$T_{\text{eff}} = 8500 \text{ K}, \log g = 2.5$ $V_t = 2 \text{ km s}^{-1}$ and $[\text{Fe}/\text{H}] = -1.5$ WIDTH		$T_{\text{eff}} = 8750 \text{ K}, \log g = 2.0$ $V_t = 2 \text{ km s}^{-1}$ and $[\text{Fe}/\text{H}] = -1.5$ MOOG
		$[\text{X}/\text{H}] \pm \sigma$	[Ele/Fe]	$[\text{X}/\text{H}] \pm \sigma$	[Ele/Fe]	$[\text{X}/\text{H}] \pm \sigma$
He I	1	$-0.55 \pm 0.20$		$-0.68 \pm 0.20$		$-1.13 \pm 0.31$
Na I	2	$-1.28 \pm 0.10$	+0.21	$-1.30 \pm 0.10$	+0.20	$-0.79 \pm 0.11$
Mg I	3	$-1.46 \pm 0.07$	+0.03	$-1.48 \pm 0.05$	+0.02	$-1.03 \pm 0.16$
Mg II	2	$-1.56 \pm 0.14$	-0.07	$-1.59 \pm 0.09$	-0.09	$-1.83 \pm 0.15$
Si II	4	$-1.10 \pm 0.15$	+0.39	$-1.20 \pm 0.12$	+0.30	$-1.31 \pm 0.24$
Ca I	2	$-0.80 \pm 0.35$	+0.69	$-0.93 \pm 0.25$	+0.57	$-0.09 \pm 0.33$
Ca II	1	$-0.49 \pm 0.10$	+1.00	$-0.62 \pm 0.10$	+0.88	$-0.32 \pm 0.10$
Sc II	7	$-0.99 \pm 0.25$	+0.50	$-1.04 \pm 0.25$	+0.45	$-0.73 \pm 0.25$
Ti II	51	$-0.75 \pm 0.18$	+0.74	$-0.83 \pm 0.25$	+0.67	$-0.59 \pm 0.19$
Cr II	8	$-1.41 \pm 0.12$	+0.08	$-1.47 \pm 0.12$	+0.03	$-1.38 \pm 0.12$
Fe I	13	$-1.48 \pm 0.15$	+0.02	$-1.53 \pm 0.26$	+0.02	$-0.99 \pm 0.14$
Fe II	28	$-1.50 \pm 0.21$	+0.00	$-1.46 \pm 0.22$	+0.02	$-1.52 \pm 0.22$
Sr II	1	$-2.19 \pm 0.10$	-0.70	$-2.21 \pm 0.10$	-0.71	$-1.65 \pm 0.12$
Y II	2	$-1.20 \pm 0.17$	+0.29	$-1.30 \pm 0.12$	+0.37	$-0.64 \pm 0.14$
Ba II	2	$-1.21 \pm 0.05$	+0.28	$-1.23 \pm 0.04$	+0.26	$-0.61 \pm 0.10$

**Table 3.** Comparison of the abundances of ZNG4 with the abundances of M13 BHB and RGB stars

Element	ZNG4 [Fe/H]= -1.49 $T_{\text{eff}} = 8500 \text{ K}$ $\log g = 2.5$	M13/ J11 (BHB) * [Fe/H]= -1.82 $T_{\text{eff}} = 7681 \text{ K}$ $\log g = 3.1$	M13/WF4-3485(BHB) * [Fe/H]= + 0.02 $T_{\text{eff}} = 12750 \text{ K}$ $\log g = 4.1$	M13/ L262 (RGB) * [Fe/H]= -1.61 $T_{\text{eff}} = 4160 \text{ K}$ $\log g = 0.50$	Mean RGB abundances * in M13
	[X/H]	[X/H]	[X/H]	[X/H]	[X/H]
He	-0.55	< -0.26	- 1.49 $\pm$ 0.17	...	...
Na	-1.28	...	...	-1.27 $\pm$ 0.11	-1.37 $\pm$ 0.04
Mg	-1.51	-1.50 $\pm$ 0.16	- 1.62 $\pm$ 0.14	-1.51 $\pm$ 0.14	-1.46 $\pm$ 0.03
Si	-1.10	< -1.23	- 1.43 $\pm$ 0.07	-1.16 $\pm$ 0.14	-1.30 $\pm$ 0.02
Ca	-0.64	-1.72 $\pm$ 0.11	- 1.66 $\pm$ 0.15	-1.39 $\pm$ 0.14	-1.34 $\pm$ 0.01
Sc	-0.99	-1.63 $\pm$ 0.10	< + 1.10	...	-1.67 $\pm$ 0.01
Ti	-0.75	-1.32 $\pm$ 0.06	- 0.53 $\pm$ 0.16	-1.30 $\pm$ 0.20	-1.32 $\pm$ 0.02
Cr	-1.41	-1.71 $\pm$ 0.12	< - 0.12	...	...
Fe	-1.49	-1.82 $\pm$ 0.10	+ 0.02 $\pm$ 0.20	-1.61 $\pm$ 0.10	-1.60 $\pm$ 0.01
Sr	-2.19	-2.03 $\pm$ 0.10	< + 1.75	...	...
Y	-1.20	< -0.97	< + 2.92	...	- 1.61 $\pm$ 0.04
Ba	-1.21	-1.68 $\pm$ 0.10	< + 3.26	...	- 1.53 $\pm$ 0.05

\* Abundances of M13 BHB stars are from Behr (2000c) and abundances of M13 RGB star are from Cavallo & Nagar (2000). In the last column, the mean abundances of elements from Na to Fe in M13 RGB stars are from Kraft et al.(1997) and that of Y and Ba are from Armosky et al. (1994).